Kinetics of the Overall Higher Alcohol Synthesis Reacting System*

L. NOWICKI** and T. OLEWSKI

Faculty of Process & Environmental Engineering, Technical University of Lodz, PL-90 924 Lodz
e-mail: nowickil@ck-sg.p.lodz.pl

Received 2 April 2002

In the kinetic models of higher alcohol synthesis developed in this study, the reaction products were treated on a lumped basis. The alcohols and hydrocarbons (unbranched alkanes) are regarded as single pseudocomponents with average carbon number chain length depending on the process variables. The lumped treatment of the kinetics seems to be valuable to get better understanding of the effect of operating variables. The advantage of such type of models is a reduced number of parameters to be estimated. Three types of the rate equations describing the formation rates of alcohols, hydrocarbons and the rate of water-gas-shift reaction were assumed. The discrimination between the proposed rate equations was based on experimental rates measured in a tank slurry reactor over a modified Cu/ZnO catalyst. The inhibiting effect of water vapour appeared to be the most important for production of alcohols and hydrocarbons.

Higher alcohol synthesis is a process of converting synthesis gas (H_2 + CO) into the mixture of C_1—C_6 alcohols, which can be used as an additive to motor fuels instead of commonly used MTBE. Fuels produced in this way are of high quality due to excellent combustion properties and reduced emissions. Synthesis gas can be produced from a variety of sources, including coal gasification, natural gas reforming, and biomass pyrolysis.

The major oxygenated product of the higher alcohol synthesis is methanol. The other alcohols are predominantly linear, although a small amount of branched ones, *e.g.* alkan-2-ols, is always formed. Depending on the catalyst used some hydrocarbons may also be formed. Hydrocarbons are mainly alkanes, although formation of alk-1-enes and branched alkanes cannot be excluded either.

During the higher alcohols synthesis three simultaneous series-parallel reactions of alcohol and n-alkanes formation and water-gas shift occur

$$n\mathrm{CO} + 2n\mathrm{H_2} \xrightarrow{r_{AL}} \mathrm{C}_n\mathrm{H}_{2n+2}\mathrm{O} + (n-1)\mathrm{H_2O} \quad (A)$$

$$m\mathrm{CO} + (2m+1)\mathrm{H_2} \xrightarrow{r_{HC}} \mathrm{C}_m\mathrm{H}_{2m+2} + m\mathrm{H_2O} \quad (B)$$

$$\mathrm{CO} + \mathrm{H_2O} \xrightleftharpoons{r_{WGS}} \mathrm{CO_2} + \mathrm{H_2} \quad (C)$$

where n and m are the average carbon chain lengths of the alcohol and hydrocarbon product, respectively. Both n and m can vary with the catalyst and process conditions. Water is generally believed to be a primary product of the alcohol and hydrocarbon reactions, and CO_2 is produced by the water-gas shift.

Catalysts for higher alcohol synthesis can be divided into two groups: methanol synthesis catalysts modified with alkali promoters, and modified Fischer—Tropsch catalysts. The water-gas shift was particularly important over the catalysts obtained by modification of typical Fischer—Tropsch catalysts. All three reactions must be considered in order to accurately correlate H_2 and CO reaction rates over this type of catalysts.

Several models for product formation during higher alcohol synthesis have appeared in the literature. In these studies kinetic models were derived from a rigorous reaction network for alcohol chain. *Smith* and *Anderson* [1] were the first to present this approach to C_{2+} alcohol product distribution over commercial $Cu/ZnO/Al_2O_3$ catalyst promoted with potassium. A mechanistic model for oxygenated products over Cs-promoted Zn/CrO_x catalysts was developed by *Tronconi et al.* [2]. Similar approach to the modelling of methanol and higher alcohols formation over Cu/ZnO-based catalysts was adopted by *Calverley* and *Smith* [3]. An attempt to model the simultaneous formation of hydrocarbons and alcohols was reported by *Xiaoding et al.* [4] for Rh-based (IFP) catalysts and by *Smith et al.* [5] and *Park et al.* [6] for MoS_2-based catalysts.

*Presented at the 29th International Conference of the Slovak Society of Chemical Engineering, Tatranské Matliare, 27—31 May 2002.

**The author to whom the correspondence should be addressed.

Breman et al. [7] made extensive study of higher alcohol synthesis over Cs-Cu/ZnO/Al_2O_3 catalyst on the basis of which they proposed the kinetic model including formation of a wide group of products, *e.g.* linear and branched alcohols and alkanes, esters, CO_2, and water.

The number of parameters appearing in the model can be reduced significantly when a lumped kinetic approach is used. In the model proposed by *Tronconi et al.* [8], C_{2+} alcohols and C_{2+} hydrocarbons were regarded as single pseudocomponents with the same average carbon number. The reaction network included reversible methanol synthesis and water-gas-shift reaction, formation of higher alcohols from methanol, hydrogenation of CO to methane, and dehydration of C_{2+} alcohols to corresponding alkenes.

The purpose of this paper is to compare different kinetic equations of the higher alcohol synthesis that can be used to describe the overall rate of hydrocarbons and alcohols formation over a modified copper/zinc catalyst. The comparison was based on experimental data of the reactor outlet flow composition (CO, H_2, and CO_2 content) and produced alcohols and alkanes carbon chain length. Copper/zinc catalysts are promising for future commercialization. Improvement of their properties is still one of the major interests in the field of the higher alcohol production. The lumped treatment of the kinetics seems to be valuable to get better understanding of the effect of the operating variables. It could also be an easy way to compare the performance of different catalysts.

A number of different types of reactors are used in the laboratory. Perfectly mixed reactors are employed for detailed kinetic studies, as the reactor is presumably free of concentration and temperature gradients facilitating the data analysis. In this study a slurry stirred tank reactor was used. It is a three-phase (gas-liquid-catalyst) reactor, similar to those commonly used for methanol and the Fischer—Tropsch syntheses [9, 10]. In the literature, the data for higher alcohol synthesis in slurry phase are rather scarce [11].

EXPERIMENTAL

The kinetic equations were tested using experimental data obtained in a 1 dm^3 stirred tank slurry reactor (Haage). The feed gas flow rate and H_2 to CO volumetric ratio were controlled using a mass flow meter for each gas. The gas inlet into the reactor was situated just beneath the flat-bladed impeller to maximize the gas shear.

After leaving the reactor, products, together with unreacted syngas, passed through high and low (ambient) pressure traps. The heated high-pressure trap was used to separate slurry liquid and the low-pressure one to condense liquid alcohols and hydrocarbons. Liquid products were analyzed by gas chromatography with FID detector. The synthesis gas components and noncondensable products leaving the ice trap (low-pressure) were analyzed on an on-line GC with two different columns and both with flame ionization and thermal conductivity detectors.

The catalyst, CuO/ZnO/ZrO_2/F_2O_3/MoO_3/ThO_2/Cs_2O was synthesized in the Institute of Chemical Engineering, Polish Academy of Sciences in Gliwice [12]. The catalyst was pretreated *in situ*, using $\varphi_r(H_2:He) = 1:20$ mixture at 493 K for 15 h and then $\varphi_r(H_2:He) = 1:4$ mixture at 493 K for 2 h. The gas space velocity (at normal conditions) during the activation was 5.9 $m^3\ kg^{-1}\ h^{-1}$.

The catalyst was tested to determine its performance during higher alcohols synthesis at different reaction conditions. However, for the purpose of this study only the isothermal data obtained at 583 K were used. The other operating conditions were as follows: pressure 4.1 and 5.6 MPa, gas space velocity 4.5—7.5 $m^3\ h^{-1}\ kg^{-1}$ (at normal conditions), and feed $\varphi_r(H_2:CO)$ ratio from 0.7 to 2.3 (Table 1). A molten wax Vestowax SH-105 (Chemische Werke Hüls) was used as a slurry liquid for the reactor tests.

Except alcohols, a significant amount of hydrocarbons (mainly alkanes) and CO_2 was formed. As shown in Fig. 1, the distribution of carbon numbers of both hydrocarbons and alcohols followed the Anderson—Schulz—Florry (ASF) distribution very well. This behaviour is typical for the Fischer—Tropsch catalysts. The strong activity towards hydrocarbons, which is not a typical behaviour of Cu/ZnO-based catalysts, may be caused by iron promoter.

The catalyst showed high water-gas-shift activity,

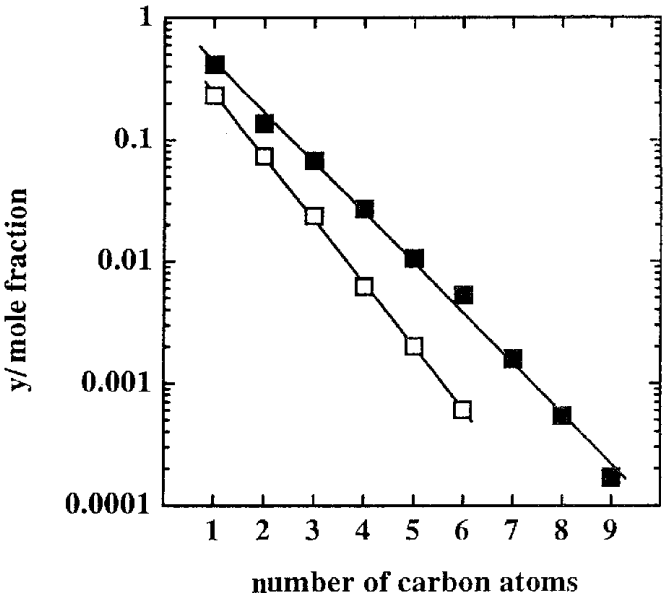

Fig. 1. Anderson—Schulz—Florry carbon number distribution for alcohols (□) and alkanes (■) at 583 K, 5.6 MPa, 4.6 $m^3\ h^{-1}\ kg^{-1}$, and feed ratio $\varphi_r(H_2:CO) = 2.2$. (The chain growth probabilities for hydrocarbons and alcohols are 0.39 and 0.30, respectively.)

Table 1. Experimental Data for Higher Alcohol Synthesis over Cu/ZnO Catalyst at 583 K

P	SV[a]	φ_r (Feed H_2:CO)	n	m	r_{AL}^{exp}	r_{HC}^{exp}	r_{WGS}^{exp}
MPa	$m^3\ h^{-1}\ kg^{-1}$				mol h^{-1} kg^{-1}	mol h^{-1} kg^{-1}	mol h^{-1} kg^{-1}
5.6	4.48	2.3	1.34	1.61	1.88	4.04	6.39
5.6	4.50	2.3	1.45	1.65	1.87	3.66	6.69
5.6	4.59	1.0	1.56	1.78	1.28	2.39	6.54
5.6	4.50	0.7	1.58	1.83	1.08	1.90	4.99
5.6	4.61	2.3	1.44	1.64	1.90	3.80	7.83
5.6	7.53	2.1	1.47	1.73	2.48	4.36	8.47
5.6	4.46	2.2	1.47	1.68	1.84	3.65	7.01
4.1	4.61	2.2	1.47	1.76	1.34	3.06	5.78
5.6	4.61	2.2	1.43	1.69	1.99	3.83	7.11
4.1	4.59	1.0	1.66	1.87	1.18	2.23	5.73
5.6	4.61	2.2	1.49	1.66	1.99	3.29	6.56

a) At normal conditions.

as majority of the water produced together with C_{2+} alcohols and hydrocarbons subsequently reacted to form CO_2.

RESULTS AND DISCUSSION

To evaluate the kinetic equation, a set of material balances for the perfectly mixed reactor was derived assuming:

1. The reactor is steady-state and the catalyst activity is constant.

2. The reactor is perfectly mixed, with uniform temperature and pressure in both the gas and liquid phases. All heat effects are ignored and the gas and liquid phase concentrations are uniform throughout each respective phase.

3. Gaseous species (CO, CO_2, H_2, and H_2O) are in equilibrium with the liquid, and the liquid is inert.

The mass balance using these assumptions for any species i is given by a simple algebraic equation

$$F_i^{in} - F_i + m_{cat} R_i = 0 \qquad (1)$$

where i = CO, H_2, CO_2, $C_nH_{2n+2}O$, C_mH_{2m+2}, H_2O. According to stoichiometry (reactions (*A*) to (*C*)) the net rates of formation of individual species R_i can be written as

$$R_{CO} = -nr_{AL} - mr_{HC} - r_{WGS} \qquad (2)$$

$$R_{H_2} = -2nr_{AL} - (2m+1)r_{HC} + r_{WGS} \qquad (3)$$

$$R_{CO_2} = r_{WGS} \qquad (4)$$

$$R_{C_nH_{2n+2}O} = r_{AL} \qquad (5)$$

$$R_{C_mH_{2m+2}} = r_{HC} \qquad (6)$$

$$R_{H_2O} = -r_{WGS} + (n-1)r_{AL} + mr_{HC} \qquad (7)$$

Solving these equations for known kinetic expressions gives the outlet molar flow rates of individual components, which can be used to calculate the corresponding partial pressures. In fact, reaction rate is a function of temperature and liquid phase concentrations in a slurry reactor; however, it is more convenient to use gas phase partial pressures in place of liquid concentrations. According to the third assumption applied in the model development, the partial pressures and liquid concentrations can be related directly: $C_i = H_i P_i$. On the other hand, the use of the liquid phase reactant concentration will affect the dimensions of the corresponding reaction rate constant.

The experimental data reported in Table 1 were fitted using the three models listed in Table 2. The first model assumes a first-order dependence of alcohols and hydrocarbon reaction rates on H_2 partial pressure and second-order mass action kinetics for water-gas-shift reaction. A first-order dependence of the Fischer—Tropsch reaction rate on H_2 partial pressure is well known from the experiment

$$r_{HC} = kP_{H_2} \qquad (8)$$

Anderson [13] found that the first-order rate equation was acceptable for H_2 and CO conversions up to 60 %.

It is believed that rate inhibition by water can occur at higher conversions for alcohols as well as hydrocarbons production. By assuming the simple kinetics adopted in the first model, any inhibition effects, if they exist, are being lumped into the numerical value of the reaction rate constant.

The second model is based on the rate expression proposed by *Anderson* [13], where the inhibition of hydrocarbon formation by water is included

$$r_{HC} = \frac{kP_{CO}P_{H_2}}{P_{CO} + aP_{H_2O}} \qquad (9)$$

Dry et al. [14] derived this equation from the enol mechanism by assuming that hydrogenation of chemisorbed CO was the rate-determining step

$$CO + \# \rightleftarrows CO\# \qquad (D)$$

Table 2. Summary of Models and Kinetic Parameter Estimates

	r_{AL}	r_{HC}	r_{WGS}
	Model 1		
Rate equation	$k_1 P_{H_2}$	$k_2 P_{H_2}$	$k_3\left(P_{CO}P_{H_2O} - \frac{P_{H_2}P_{CO_2}}{K_P}\right)$
k_i/(mol h^{-1} MPa^{-1} kg^{-1})	0.62	1.21	9.32[a]
NRMSE	0.062	0.068	0.235
	Model 2		
Rate equation	$\frac{k_1 P_{CO} P_{H_2}}{P_{CO} + b_1 P_{H_2O}}$	$\frac{k_2 P_{CO} P_{H_2}}{P_{CO} + b_2 P_{H_2O}}$	$\frac{k_3\left(P_{CO}P_{H_2O} - \frac{P_{H_2}P_{CO_2}}{K_P}\right)}{P_{CO} + b_3 P_{H_2O}}$
k_i/(mol h^{-1} MPa^{-1} kg^{-1})	0.51	0.99	420
b_i	1×10^{-4}	8×10^{-5}	125
NRMSE	0.032	0.040	0.129
	Model 3		
Rate equation	$\frac{k_1 P_{CO} P_{H_2}}{P_{CO} + a_1 P_{CO_2}}$	$\frac{k_2 P_{CO} P_{H_2}}{P_{CO} + a_2 P_{CO_2}}$	$\frac{k_3\left(P_{CO}P_{H_2O} - \frac{P_{H_2}P_{CO_2}}{K_P}\right)}{P_{CO} + a_3 P_{CO_2}}$
k_i/(mol h^{-1} MPa^{-1} kg^{-1})	0.60	1.09	30.0
a_i	0.39	0.001	0.001
NRMSE	0.051	0.042	0.220

a) In mol h^{-1} MPa^{-2} kg^{-1}.

$$CO\# + H_2 \longrightarrow COH_2\# \qquad (E)$$

where # denoted an active site on the catalyst surface. The authors assumed Langmuirian adsorption and considered competitive adsorption of CO, CO_2, H_2, and H_2O. Moreover, the following assumption was taken into account, $K_{CO}P_{CO} + K_{H_2O}P_{H_2O} \gg 1 + K_{CO_2}P_{CO_2} + K_{H_2}P_{H_2}$, in order to get the reaction rate expression for the hydrocarbons formation; $a = K_{H_2O}/K_{CO}$.

The inhibitory effect of water vapour on higher alcohols formation was assumed by *Tronconi et al.* [8], resulting in the rate expression

$$r_{AL} = \frac{kP_{CH_3OH}}{1 + K_{H_2O}P_{H_2O}} \qquad (10)$$

Only a few studies of higher alcohol synthesis including the water-gas-shift reaction kinetics have been reported in the literature [6, 8, 15]. *Tronconi et al.* [8] applied the rate equation

$$r_{WGS} = k\left(P_{CO}P_{H_2O} - \frac{P_{H_2}P_{CO_2}}{K_P}\right) \qquad (11)$$

where a simple second-order mass action kinetics was assumed. On the other hand, in the kinetic study of *Park et al.* [6] the first-order reversible kinetics for the CO_2 formation by water-gas-shift reaction was used

$$r_{WGS} = k\left(P_{CO} - \frac{P_{CO_2}}{K_P}\right) \qquad (12)$$

However, for the second model, the reaction rate expression

$$r_{WGS} = \frac{k(P_{CO}P_{H_2O} - P_{CO_2}P_{H_2}/K_P)}{P_{CO} + aP_{H_2O}} \qquad (13)$$

proposed by *Leib* and *Kuo* [15] was adopted.

In the third model used in this study, the inhibition by CO_2 was assumed. Therefore, in all rate equations the water partial pressure in the denominator was replaced by the partial pressure of this component.

Inhibition by CO_2 is generally not as strong as inhibition by water due to the large adsorption coefficients of water relative to CO and CO_2. However, CO_2 inhibition may become important when a large fraction of the water produced by the reactions (A) and (B) reacts with CO to produce CO_2 *via* the water-gas shift. *Ledakowicz et al.* [16] derived a rate expression that incorporated inhibition by CO_2 from the enol mechanism, but assumed that CO_2 and CO were the dominant terms in the denominator of the Langmuir—Hinselwood equation obtained.

The term K_P represents the equilibrium constant of the water-gas-shift reaction. According to *Newsome* [17], the temperature dependence of K_P could be expressed as follows

$$K_P = 0.0132\exp(4577.8/T) \qquad (14)$$

This equation was used to calculate the corresponding value at the reaction temperature of 583 K.

Due to the correlation between water and CO_2 partial pressures, those rate models which account for either water or CO_2 inhibition alone were considered.

The nonlinear least-squares regression was used to obtain the parameter estimates that were constrained to be greater than zero in all cases. The objective function used in the model parameters evaluation was the normalized root mean square error (NRMSE)

$$\mathrm{NRMSE} = \sum_{i=\mathrm{AL,HC,WGS}} \left(\frac{1}{N} \sqrt{\sum_{j=1}^{N} \left(\frac{r_{ij}^{\mathrm{exp}} - r_{ij}^{\mathrm{calc}}}{r_{ij}^{\mathrm{exp}}} \right)^2} \right) \quad (15)$$

where N is the number of experiments. For each model, the optimum values of kinetic parameters and their contribution to the NRMSE are given in Table 2.

For alcohols formation, models 1 and 3 gave an equally good fit of experimental data, with an NRMSE of 0.05—0.06. The best results were obtained for the kinetic model assuming the inhibition by H_2O, with an NRMSE of 0.032. For the Fischer—Tropsch reaction again the best fit for model 2 was found, with NRMSE of 0.040, although very similar results for model accounting for CO_2 inhibition were obtained. Significantly better fit of the CO_2 formation *via* water-gas-shift reaction was obtained for the model 2 (NRMSE = 0.129) compared to simulation by the models 1 and 3 (NRMSE = 0.235 and 0.220, respectively). Thus, in the higher alcohol synthesis, the inhibitory effect of H_2O on alcohol, hydrocarbon formation rates as well as on water-gas-shift reaction rate seems to be important.

In the case of the kinetic model 2, estimated value of the parameter b_3 (water-gas-shift reaction) was much larger compared to the values of parameters b_1 and b_2 obtained for alcohols and hydrocarbons formation, respectively. It means a very strong inhibiting effect of water partial pressure on water-gas-shift reaction.

Fig. 1 presents the Anderson—Schulz—Florry carbon number distribution of the products. The found probability of chain growth (reflected by tne slope of ASF plot) was different for alcohols and hydrocarbons, which means that their formation occurred independently. Therefore, the presence of different catalyst active centres responsible for alcohols and hydrocarbons production is probable.

If the two reactions proceed through different surface species or occur on different catalytic sites, the adsorption constants of species adsorbed on active centres of different nature are not expected to have the same numerical values. However, for model 2 the values of parameters b_1 and b_2, a measure of H_2O adsorption strength, are very similar for alcohols and hydrocarbons formation.

Since in the case of higher alcohol catalysts a high activity towards hydrocarbons is accompanied by a high activity of water-gas-shift reaction, it seems that these two reactions should have similar a or b estimates, which is the case for the parameter a in model 3 only. It may suggest that these two reactions proceed through different mechanisms. However, if this is the case, there is no reason to assume that the functional form of the denominators will be the same. Unfortunately, very little information has appeared in literature concerning simultaneous Fischer—Tropsch, higher alcohol, and water-gas-shift kinetics, and the proper form of the rate equation is not clear.

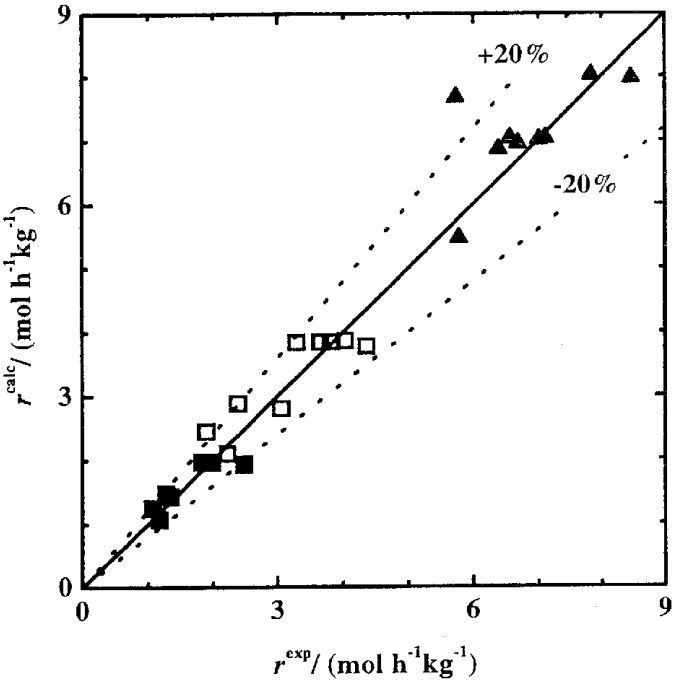

Fig. 2. Parity plots for alcohols (■), hydrocarbons (□) formation and water-gas-shift (▲) reactions according to the model 2.

Although the NRMSE for CO_2 formation rates is higher than for alcohols and hydrocarbons, the parity plot presented in Fig. 2 shows that model 2 fits all experimental data reasonably well. The agreement for water-gas-shift reaction is very satisfactory except one of the points that is out of 20 % of its measured value.

SYMBOLS

a, b	model parameter	
C	molar concentration	mol m^{-3}
F	molar flow rate	mol s^{-1}
H	Henry' s constant	
K_P	water-gas-shift reaction equilibrium constant	
k	rate constant (see Table 2)	mol h^{-1} MPa^{-1} kg^{-1}
m	average carbon number in hydrocarbon molecule	
m_{cat}	mass of catalyst	kg
N	number of experiments	

n	average carbon number in alcohol molecule	
P	partial pressure	MPa
R	rate of formation	mol h^{-1} kg^{-1}
r	reaction rate	mol h^{-1} kg^{-1}
SV	space velocity	m^3 h^{-1} kg^{-1}

Subscripts

AL	reaction for alcohols
HC	Fischer—Tropsch reaction for hydrocarbons
i	component i
j	j-th experiment
WGS	water-gas-shift reaction

Superscripts

in	inlet
exp	determined experimentally
calc	calculated

REFERENCES

1. Smith, J. and Anderson, R. B., *J. Catal. 85*, 428 (1984).
2. Tronconi, E., Lietti, L., Forzatti, P., Groppi, G., and Pasquon, I., *Catal. Sci. Technol. 1*, 255 (1991).
3. Calverley, E. M. and Smith, K. J., *Ind. Eng. Chem. Res. 31*, 792 (1992).
4. Xiaoding, X., Doesburg, E. B. M., and Scholten, J. J. F., *Catal. Today 2*, 125 (1987).
5. Smith, K. J., Herman, R. G., and Klier, K., *Chem. Eng. Sci. 45*, 2639 (1990).
6. Park, T. Y., Nam, I.-S., and Kim, Y. G., *Ind. Eng. Chem. Res. 36*, 5246 (1997).
7. Breman, B. B., Beenackers, A. A. C. M., and Osterholt, E., *Chem. Eng. Sci. 49*, 4409 (1995).
8. Tronconi, E., Forlazzo, N., Forzatti, P., and Pasquon, I., *Ind. Eng. Chem. Res. 26*, 2122 (1987).
9. Cybulski, A., *Catal. Rev.—Sci. Eng. 36*, 557 (1994).
10. Davies, B. H., *Catal. Today 71*, 249 (2002).
11. Breman, B. B., Beenackers, A. A. C. M., Schurman, H. A., and Osterholt, E., *Catal. Today 24*, 5 (1995).
12. *Pol.* P303523 (1994).
13. Anderson, R. B., *Catalysis.* Vol. *IV.* (Emmett, P. H., Editor.) Van Nostrand Reinhold, New York, 1956.
14. Dry, M. E., Shingles, T., and Boshoff, L. J., *J. Catal. 25*, 99 (1972).
15. Leib, T. B. and Kuo, J. S. W., "Modelling the Fischer—Tropsch Synthesis in Slurry Bubble-Column Reactors", *AIChE Annual Meeting*, San Francisco, 1984.
16. Ledakowicz, S., Nettelhoff, H., Kokum, R., and Deckwer, W.-D., *Ind. Eng. Chem., Process Des. Dev. 24*, 1043 (1985).
17. Newsome, D. S., *Catal. Rev.—Sci. Eng. 21*, 275 (1980).